

A deep learning approach to the study of colloidal microparticles assembly process in three-dimensional space

© I.V. Simkin, A.A. Shirokova, A.I. Shvetsov, A.V. Kohanovskaya, P.A. Zabavina,
A.A. Bondareva, P.A. Libet, N.P. Kryuchkov, E.V. Yakovlev

Bauman Moscow State Technical University, Moscow, Russia
E-mail: vanyasimkin@gmail.com

Received May 3, 2024

Revised July 15, 2024

Accepted October 30, 2024

We present a deep learning-based approach to visualize and analyze the three-dimensional self-assembly of microparticles in a fluid using laser-plane microscopy, followed by coordinate reconstruction in three dimensions. A YOLOv8 neural network was employed for this purpose. It has been demonstrated that the proposed post-processing technique allows for the detection of characteristic features in the scattering pattern of microparticles with a mean average precision of 0.93, as well as the extraction of their coordinates in three-dimensional space with an accuracy of up to 20% of their diameter. This approach holds promise for controlling the self-assembly processes of microparticles in three dimensions and has the potential for enhancing the development of novel materials and technologies, such as three-dimensional bioprinting and micro- and nanoscale fabrication.

Keywords: soft matter, colloids, three-dimensional self-assembly, plane microscopy.

DOI: 10.61011/TPL.2024.12.60366.6616k

The study of self-assembly of two-dimensional structures from micro- and nanoparticles with the use of external control fields is a topical area of condensed matter physics research [1–3]. Discoveries in this field have led to significant advances in materials science [4], colloid chemistry [5], etc. Three-dimensional self-assembly is a further evolution of two-dimensional one. Studies into the processes occurring in three-dimensional self-assembly, such as the examination of diffusion processes in glasses [6,7], analysis of the kinetics of phase transitions [8,9], etc., are of key importance. They open up new opportunities in various fields. For example, this may contribute to the development of 3D bioprinting and the fabrication of tissues and organs in medicine [10–14] and the formation of complex three-dimensional micro- and nanostructures with unique properties [15,16].

The development of methods for visualization of three-dimensional self-assembly of microparticles opens up new possibilities for regulating this process. Specifically, the use of plane microscopy with a time resolution of 30 frames per second makes it possible to record dynamic self-assembly processes proceeding on a time scale on the order of 10s (the characteristic diffusion time of microparticles in a solvent), allowing one to perform particle-resolved studies of various self-assembly mechanisms in external control fields. Post-processing algorithms, including those based on machine learning methods, are needed to analyze the physical parameters of the system and determine their relation to the impact of an external control field. It should be noted that machine learning has already been applied to characterization of stochastic and nonlinear behavior of three-dimensional self-assembly systems obtained by modeling [17].

Visualization of self-assembly of experimental 3D systems presents significant difficulties. To avoid loss of data on proceeding processes, one needs to detect particles synchronously throughout the entire volume. Studies into the determination of position of a particle based on holographic analysis of colloidal particles with the use of the Lorenz–Mie scattering theory in transmitted laser light have already been published [18]. Our experimental design differs in that scattering is recorded perpendicular to the plane of propagation of the laser beam. Therefore, a different approach to particle detection is required.

The diagram of the experimental setup is presented in Fig. 1, *a*. A sheet laser with emission wavelength $\lambda = 660$ nm was used as a radiation source. The sample consisted of calibrated polystyrene microparticles $10.55 \mu\text{m}$ in diameter with a mean-square diameter deviation of $0.09 \mu\text{m}$ (PS Microparticles GmbH, Germany) dispersed in a solvent. The mass fraction of microparticles was 0.01%. A mixture of deionized water and glycerol (with a glycerol mass fraction of 10%) was chosen as a solvent. Glycerol was added to compensate for the density of the solvent relative to the density of particles and balance the Archimedes force and the force of gravity acting on a particle.

The experimental procedure was as follows: (1) the suspension was placed in a cuvette; (2) the cuvette with the sample was mounted in the laser irradiation region (the laser source was shifted to adjust the distance between it and the sample so that the latter was in the laser beam waist); (3) the vertical position of the region of intersection between the laser beam and the sample (laser sheet) was set so that a microparticle was positioned in the most intense region of laser beam propagation (the *XY* plane in which the central axis of the laser beam lay). This plane is perpendicular to

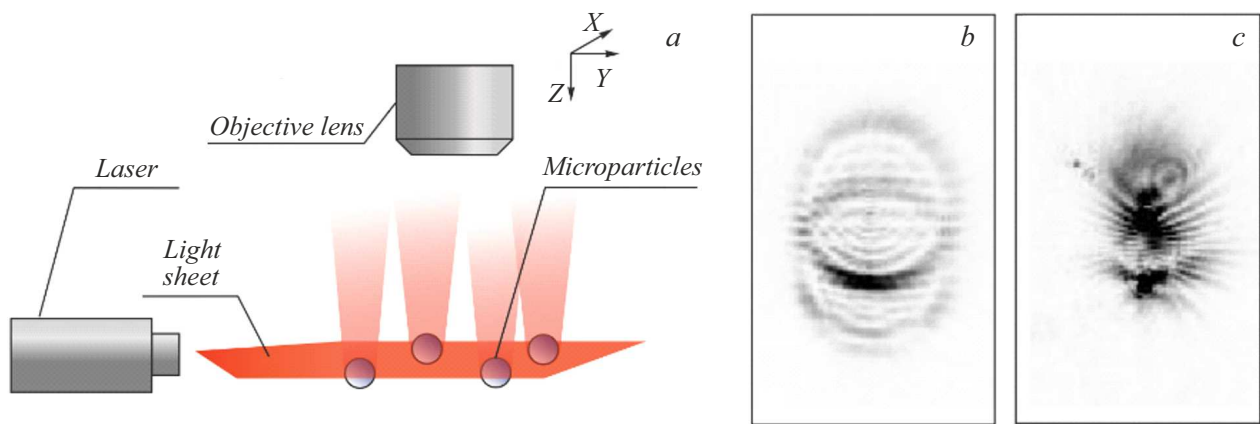


Figure 1. *a* — Schematic diagram of the plane microscopy experiment. The plane of laser beam propagation (the plane with coordinates XY in which particles are observed; shown in red) and the optical axis of the lens (coordinate Z) are orthogonal. A color version of the figure is provided in the online version of the paper. *b, c* — Patterns of scattering of a laser beam off the same particle (colors inverted) located below (*b*) and above (*c*) the focal plane of the camera.

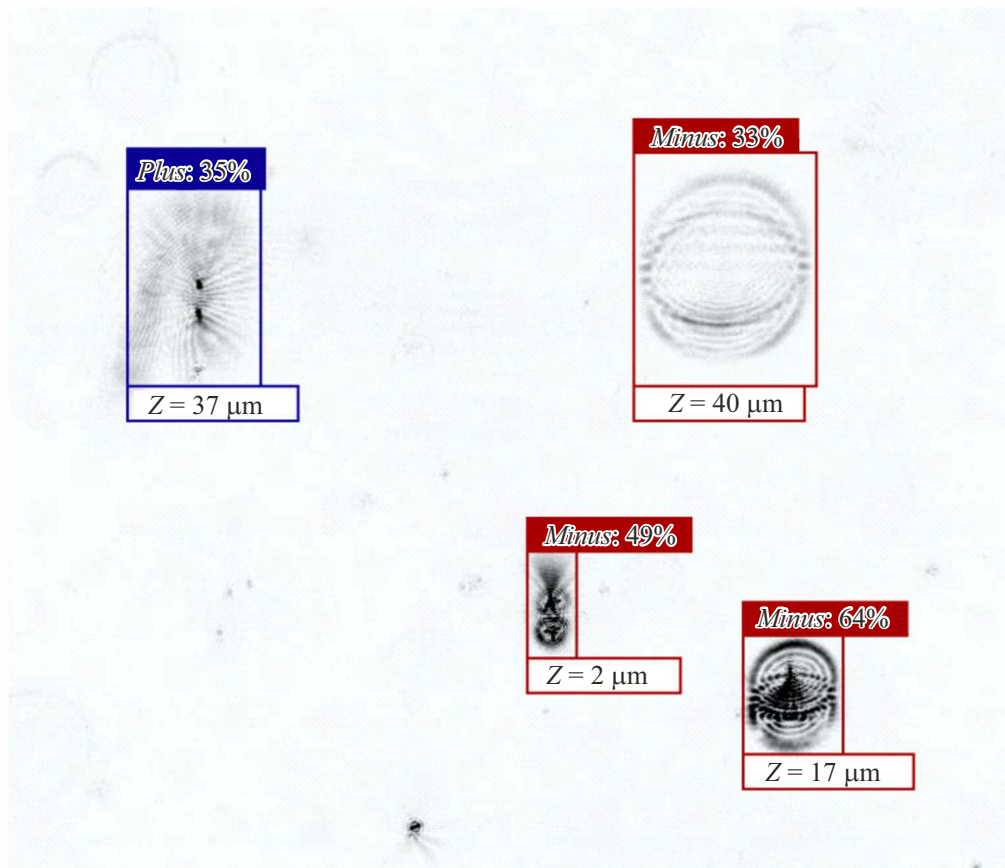


Figure 2. Result of determination of coordinate Z of colloidal microparticles. Particles above the focal plane are marked in blue and labeled „Plus“, while particles below the focal plane are marked in red and labeled „Minus“. The absolute value of coordinate Z of the particle center is indicated below. A color version of the figure is provided in the online version of the paper.

the optical axis of the camera, which coincided with the Z coordinate direction. The vertical position of the microscope was also adjusted so that a microparticle remained in the focal plane of the optical system.

The approach to detection of microparticles in volume is based on the fact that the characteristic scattering pattern of a laser beam scattered by particles depends on their position relative to the focal plane of the camera. Figures 1, *b* and

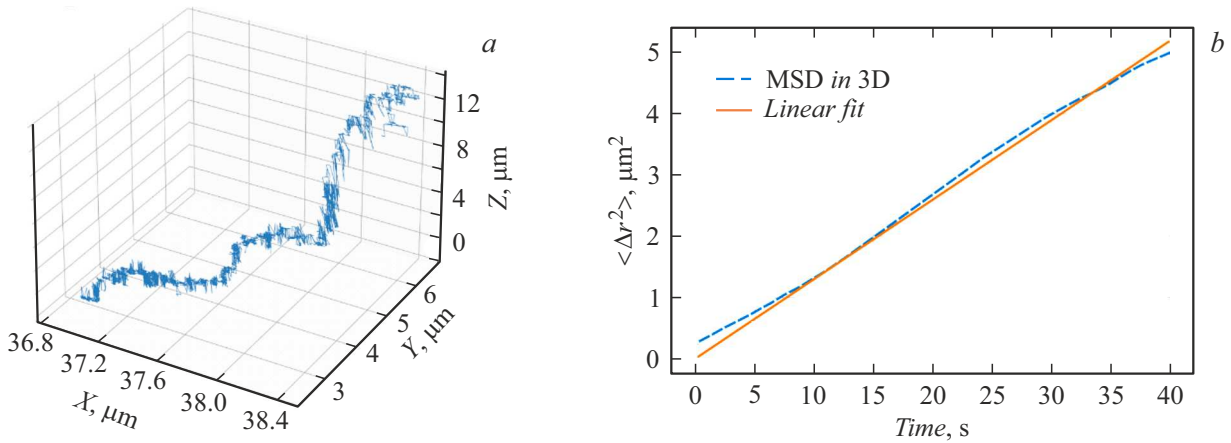


Figure 3. *a* — Three-dimensional trajectory of a colloidal microparticle in a solvent reconstructed using the post-processing algorithm. *b* — Calculated mean-square displacement of particles as function of the observation time (dashed curve) and approximation of the dependence by a linear function (solid curve).

c present the patterns of scattering below and above the focal plane, respectively.

The YOLOv8 [19] neural network was trained to detect microparticles based on laser beam scattering patterns. The YOLOv8 architecture includes multiple convolution, pooling, and fully connected layers, providing a high accuracy of object detection. The training dataset consisted of 848 images (with a resolution of 1600×1120 pixels). The labeling of images for training was performed manually in the LabelImg [20] program. Rectangular frames (bounding boxes) were used to highlight regions of the scattering pattern that corresponded to different positions of microparticles relative to the focal plane of the lens. The trained neural network detects regions of the particle scattering pattern with a mean average precision of 0.93. Figure 2 presents the result of training the YOLOv8 neural network. „Plus“ particles (above the focal plane) are marked in blue, while „Minus“ particles (below the focal plane) are marked in red. Coordinates X and Y corresponding to the coordinates of particle centers in the plane of detection by the camera were defined as the coordinates of the centers of the corresponding bounding boxes.

Relying on detection, the neural network extracts characteristic features of the scattering pattern, such as its size, shape, and position of the center of mass. To determine the Z coordinate, one needs to establish a correspondence between the scattering pattern features and the absolute coordinate. Particle parameters obtained from calibration measurements were used as absolute values of coordinates Z .

The series of calibration measurements included 50 measurements at different positions of the laser beam along the Z axis. A microparticle was initially located at the center of intensity of the laser plane and in the focal plane of the optical system. In the course of the experiment, the vertical position of the optical observation system was adjusted using a mechanical translation stage

with $5 \mu\text{m}$ steps (i.e., within the range of $250 \mu\text{m}$). The microparticle was photographed at each step. A total of 20 series of this kind with 40 measurements in each were performed. These measurements provided visual images of laser radiation scattered off particles at various distances from the microparticle to the working plane of the chamber.

Thus, data on the dependence of the shape of the scattered radiation pattern for the microparticle on its vertical position along the Z axis relative to the center of the laser beam propagation plane and the focusing plane of the optical system of the camera in which particles are observed with the greatest clarity and accuracy (the working plane of the optical system) were collected. The scattering pattern has its individual features and contains information about the vertical position of the particle along the Z axis, which was later used to develop a method for detection of particles, determination of their coordinates, and plotting of their trajectories.

The trajectories of particles were determined based on their obtained coordinates (X, Y, Z ; see Fig. 3, *a*). The mean-square displacements of particles in the solvent were then calculated. The dashed curve in Fig. 3, *b* represents the averaged mean-square displacement for 108 particles that propagated freely in the medium. The solid curve in Fig. 3, *b* corresponds to linear approximation $\langle \Delta r^2 \rangle = 4Dt$, where D is the diffusion coefficient. According to this approximation, the diffusion coefficient is $1.18 \cdot 10^{-14} \text{ m}^2/\text{s}$. This result is consistent with the diffusion coefficient calculated using the Stokes–Einstein formula:

$$D = \frac{RT}{3\pi\eta\sigma N_A} \approx 1.63 \cdot 10^{-14} \text{ m}^2/\text{s}, \quad (1)$$

where $R = 8.31 \frac{\text{m}^2 \cdot \text{kg}}{\text{s}^2 \cdot \text{K} \cdot \text{mol}}$ is the universal gas constant, $T = 293 \text{ K}$ is the absolute temperature, $\eta = 2.49 \cdot 10^{-3} \text{ Pa} \cdot \text{s}$ is the dynamic viscosity of the solvent (determined in accordance with the formula for the dynamic viscosity of a mixture of liquids proposed by

Arrhenius), $\sigma = 10.55 \mu\text{m}$ is the colloidal particle diameter, and $N_A = 6.02 \cdot 10^{23}$ is the Avogadro number.

The results of processing of experimental data for drifting microparticles in the solvent demonstrate that our algorithm has the capacity to reconstruct the coordinates of particles (X, Y, Z) along the focal axis of the lens within $\pm 80 \mu\text{m}$.

The ability to control and regulate the processes of self-assembly of microparticles in three-dimensional space at the level of individual particles holds promise for further advances in the field of fabrication of novel functional materials and for control of the dynamics of self-assembly, design of new materials with unique properties, and development of innovative technologies in micro- and nanofabrication.

Funding

This study was carried out with support from the Russian Science Foundation (grant No. 22-72-10128) at the Bauman Moscow State Technical University.

Conflict of interest

The authors declare that they have no conflict of interest.

References

- [1] N.A. Dmitryuk, L.A. Mistryukova, N.P. Kryuchkov, S.A. Khrapak, S.O. Yurchenko, *Sci. Rep.*, **13** (1), 2815 (2023). DOI: 10.1038/s41598-022-26390-w
- [2] E.N. Tsiok, Y.D. Fomin, E.A. Gaiduk, E.E. Tareyeva, V.N. Ryzhov, P.A. Libet, N.A. Dmitryuk, N.P. Kryuchkov, S.O. Yurchenko, *J. Chem. Phys.*, **156** (11), 114703 (2022). DOI: 114703.10.1063/5.0075479
- [3] E.V. Yakovlev, N.P. Kryuchkov, S.A. Korsakova, N.A. Dmitryuk, P.V. Ovcharov, M.M. Andronic, I.A. Rodionov, A.V. Sapelkin, S.O. Yurchenko, *J. Coll. Interface Sci.*, **608**, 564 (2022). DOI: 10.1016/j.jcis.2021.09.116
- [4] M. Nishizawa, in *Nanocarbons for energy conversion: supramolecular approaches*, ed. by N. Nakashima. Ser. Nanostructure Science and Technology (Springer, Cham, 2019), p. 351–370. DOI: 10.1007/978-3-319-92917-0_15
- [5] C.K. Wong, X. Qiang, A.H. Müller, A.H. Gröschel, *Prog. Polymer Sci.*, **102**, 101211 (2020). DOI: 10.1016/j.progpolymsci.2020.101211
- [6] V. Carrasco-Fadanelli, Y. Mao, T. Nakakomi, H. Xu, J. Yamamoto, T. Yanagishima, I. Buttinoni, *Soft Matter*, **20** (9), 2024 (2024). DOI: 10.1039/D3SM01320K
- [7] K.A. Rose, M. Molaie, M.J. Boyle, D. Lee, J.C. Crocker, R.J. Composto, *J. Appl. Phys.*, **127** (19), 191101 (2020). DOI: 10.1063/5.0003322
- [8] A. Basu, L.B. Okello, N. Castellanos, S. Roh, O.D. Velev, *Soft Matter*, **19** (14), 2466 (2023). DOI: 10.1039/D3SM00090G
- [9] Y. Li, Q. Fan, X. Wang, G. Liu, L. Chai, L. Zhou, J. Shao, Y. Yin, *Adv. Funct. Mater.*, **31** (19), 2010746 (2021). DOI: 10.1039/D3TC02586A
- [10] K. Yan, K. Zhou, X. Guo, C. Yang, D. Wang, *Surf. Coat. Technol.*, **477**, 130347 (2024). DOI: 10.1016/j.surfcoat.2023.130347
- [11] S. Lantean, I. Roppolo, M. Sangermano, M. Hayoun, H. Dammak, G. Rizza, *Add. Manuf.*, **47**, 102343 (2021). DOI: 10.1016/j.addma.2021.102343
- [12] J.J. Martin, B.E. Fiore, R.M. Erb, *Nature Commun.*, **6** (1), 8641 (2015). DOI: 10.1038/ncomms9641
- [13] Y. Kim, H. Yuk, R. Zhao, S.A. Chester, X. Zhao, *Nature*, **558** (7709), 274 (2018). DOI: 10.1038/s41586-018-0185-0
- [14] M. Wang, J. Liu, R. Deng, J. Zhu, *Fundam. Res.*, in press (2024). DOI: 10.1016/j.fmre.2023.12.018
- [15] S. Li, J. Tang, Y. Liu, J. Hua, J. Liu, *Compos. Sci. Technol.*, **249**, 110493 (2024). DOI: 10.1016/j.compscitech.2024.110493
- [16] C. Liu, X. Feng, S. Liu, G. Lin, Z. Bai, L. Wang, K. Zhu, X. Li, X. Liu, *J. Mater. Sci. Technol.*, **168**, 194 (2024). DOI: 10.1016/j.jmst.2023.06.007
- [17] J. O’Leary, R. Mao, E.J. Pretti, J.A. Paulson, J. Mittal, A. Mesbah, *Soft Matter*, **17** (4), 989 (2021). DOI: 10.1039/D0SM01853H
- [18] M.D. Hannel, A. Abdulali, M. O’Brien, D.G. Grier, *Opt. Express*, **26** (12), 15221 (2018). DOI: 10.1364/OE.26.015221
- [19] G. Jocher, A. Chaurasia, J. Qiu, *Ultralytics YOLOv8 (8.0.0)* [Computer software] (2023). <https://github.com/ultralytics/ultralytics>
- [20] D. Tzutalin, *LabelImg* [Computer software] (2015). <https://github.com/tzutalin/labelImg>

Translated by D.Safin